Accepted for publication in Polymer Engineering and Science
Published in April, 2014
DOI: 10.1002/pen.23605

Curing, Gelling, Thermomechanical and Thermal Decomposition Behaviors of Anhydride-Cured Epoxy (DGEBA)/Epoxidized Soybean Oil (ESO) Compositions

J. Karger-Kocsis[1,2*], S. Grishchuk[3] and L. Sorochynska[3]

1- MTA–BME Research Group for Composite Science and Technology, Muegyetem rkp. 3, H-1111 Budapest, Hungary
2- Department of Polymer Engineering, Faculty of Mechanical Engineering, Budapest University of Technology and Economics, H-1111 Budapest, Hungary
3- Institut für Verbundwerkstoffe GmbH (Institute for Composite Materials), Kaiserslautern University of Technology, POBox 3049, D-67653 Kaiserslautern, Germany

Submitted to Polym. Eng. Sci., October, 2012

To whom correspondence should be addressed: karger@pt.bme.hu

Abstract

The present work was aimed at studying the effects of incorporation of epoxidized soybean oil (ESO) in a standard bisphenol A–type epoxy resin (EP) cured by anhydride hardener. The EP/ESO ratio was set for 100/0, 75/25, 50/50, 25/75 and 0/100 (wt.%/wt.%). The investigations performed covered the curing, rheology (gelling), thermomechanical (TMA) and thermogravimetric analysis (TGA) of the EP/ESO compositions. The results showed that the dilution of EP with ESO was accompanied with marked changes in the curing, gelling behavior and final properties. Differential scanning calorimetry (DSC) revealed that the crosslinking of EP/ESO≥50/50 occurred in two steps. This has been considered for the cure schedule set. The gel time of EP/ESO, determined at T=100, 120, 140 °C, respectively, increased with increasing ESO content. The activation energy of gelling increased with increasing ESO content. The glass transition temperature decreased with increasing ESO content of the transparent samples. According to TMA the coefficient of thermal expansion in the glassy state increased with increasing ESO content but was independent of the latter in the rubbery stage. TGA indicated that with increasing ESO content the thermal degradation started earlier and the char yield decreased. The Ozawa, Flynn and Wall (OFW) approach was adapted to TGA tests to calculate

the activation energy of thermal degradation. The activation energy depended on the ESO content of the EP/ESO blends and also on their actual decomposition stage. The latter means a limitation for the OFW approach.

Key words: Epoxy resin, epoxidized soybean oil, curing, chemorheology, thermal behavior, thermal decomposition

1. INTRODUCTION

Nowadays, considerable research efforts are undertaken to use renewable feedstock for the synthesis of polymers. This direction is mostly fuelled by: i) Growing awareness of environmental issues ("greenhouse effect", "carbon footprint" etc.), and ii) Depletion of crude oil associated with price rise.

Plant or vegetable oils are promising raw materials for polymer synthesis [1], and especially for the synthesis of crosslinkable thermosetting resins [2]. Vegetable oils can be provided with different functional groups by exploiting the reactivity of their inherent double bonds [3]. It is worth of mentioning that the production of vegetable oils has also societal impact because i) People can be employed for crops cultivation, ii) Polluted soils may be remediated by plantation, and iii) Gen-manipulated plants, whose crops are not accepted by the consumers, may be used. The partial replacement of common petroresins by functionalized plant oils can be treated as the first step of the "greening strategy" with resins [4-5]. A large body of works has been devoted to study selected properties of epoxy (EP) resins blended with epoxidized vegetable oils (EVO) as reviewed recently [6]. The first reports on EP/epoxidized soybean oil (ESO) blends are dated back to the 1960's [7].

For the curing of the EP/EVO blends all conventional epoxy curing agents have been tried. Amine curing of EP blends wit EVOs often resulted in phase-separated systems which exhibited improved toughness [8]. The amine curing caused phase separation in EP/EVO blends, with and without preparation of a prepolymer by reacting the amine with EVO (mostly ESO), became a favored tool of the toughness tailoring of EPs [9-10]. EVO, being a reactive modifier, worked well as viscosity regulator for EP resins, as well [11]. Miyagawa et al [12] mixed EP with ESO and epoxidized linseed oil (ELO), added them up to 50 wt.%, and cured the corresponding formulations with anhydride. Unlike to the EP/ELO blends, the EP with 30 wt.% ESO showed a two-phase structure and thus also enhanced Izod impact strength compared to the neat EP. Gupta et al [13] noticed for phtalic anhydride cured ESO/EP blends a single glass transition temperature (T_g) peak that shifted toward higher temperatures with increasing EP amount (added up to 30 parts per hundred resin, phr). Parallel to that the stiffness and strength were improved, however, at cost of elongation and impact strength. Altuna et al [14] in a recent paper studied the anhydride curing of diglycidyl ether bisphenol A-type EP (DGEBA)/ESO blends in the whole composition range. All blends were transparent. The Tg was reduced similar to the stiffness, assessed by dynamic-mechanical thermal analysis (DMTA), with increasing ESO content of the blends. On the other hand, the impact properties changed marginally as a function of the

composition. DGEBA/EVO formulations in a broad composition range were cured also by cationic mechanisms usig thermally latent catalyst [15].

Beside of the EP/EVO compositions, efforts were devoted to study the curing of the neat EVOs, as well. Though some works used amine hardeners [16-17], in most of the studies anhydrides [7,17-20], and cationically acting latent curatives [21] were used.

The works performed until now were focused mostly on the curing, mechanical and DMA properties of selected EP/EVO blends. Albeit the gelling and thermomechanical properties of EP/EVO systems are of great practical relevance, these were addressed only in few works [15, 21]. Therefore the aim of this work was to study the basic curing, rheological (gelling), thermomechanical and thermal decomposition behaviors of hybrids composed of a bifunctional EP resin (DGEBA-type) and ESO in the whole composition range. The related blends were cured by an anhydride compound in presence of catalyst.

2. EXPERIMENTAL

2.1. Materials

The EP resin with the trade name Araldite LY 5082 (Huntsman Advanced Materials, Basel, Switzerland) is a DGEBA-based EP with the following characteristics: density at 23 ^{o}C= 1.10-1.15 g/cm^3, viscosity at 25 ^{o}C= 1.7-2.2 Pa.s, epoxy content: 4.6-4.9 equ/kg (i.e. epoxy equivalent weight is: 217.4-204.1 g/equ). The ESO under the tradename of Vikoflex 7170 was a commercial product donated by Arkema (Blooming Prairie, MN, USA). Its major characteristics are: oxirane content: 7.1%, iodine value: 1.3, acid value: 0.1. The oxirane content means the oxirane (epoxy) oxygen content. Assuming 1000 g/mol for the molecular weight of ESO the above oxirane value corresponds to 4.44 epoxy groups per ESO molecule. Accordingly, the epoxy equivalent weight of ESO is 225.2 g/equ. Note that this value is very closely matched to that of the DGEBA used. Considering the fact that the different data are available for the molecular weight of soybean oil, and the epoxy equivalent weight of DGEBA and ESO are practically the same, the EP, ESO and EP/ESO combinations were cured by the same amount of hardener (i.e. the stoichiometry was not adjusted). The anhydride curing agent was Aradur 917 CH, kindly provided by Huntsman Advanced Materials (Basel, Switzerland). It has the following characteristics: density at 25 ^{o}C= 1.2-1.25 g/cm^3, viscosity at 25 ^{o}C= 50-100 mPa.s. Aradur 917 CH is composed of methyl tetrahydrophthalic anhydride (mostly) and tetrahydrophthalic anhydride. The molecular weight (MW) of the former compound is: 152.15 g. Hardening with this anhydride was accelerated by 1-methylimidazole (Accelerator DY 070; also from Huntsman) with the following characteristics: density at 25 ^{o}C= 0.95-1.05 g/cm^3, viscosity at 25 ^{o}C $\leq$ 50 mPa.s. Its amount in anhydride curable EPs is usually at about 1 wt.%. Altuna et al [14] set its amount for 3 wt.% based with respect to the anhydride content. An internet literature search confirmed that the usual composition of DGEBA-based EPs with this hardening system

is: EP(DGEBA) : Aradur 917 CH : DY 070= 100:90:1. Instead of the latter we have selected the following: 100:90:2.5 and kept constant for all systems studied. It is noteworthy that this ratio contains some anhydride surplus with respect to the stoichiometry.

The materials tested were: EP reference, EP/ESO combinations with the following ratios: 75/25, 50/50 and 25/75, ESO reference. For curing of bulk samples the following cure regimes have been selected based upon differential scanning calorimetric (DSC) results (disclosed later): 2 h at T=100 ºC, 2 h at T=140 ºC and 2 h at T= 180 ºC (referred to steps I, II and III, respectively). Curing of the samples, placed in containers produced from tin plates, was performed in a programmable thermostatic oven.

2.2. Tests

Differential scanning calorimetry (DSC)

Dynamic (temperature ramp) scans were performed on the cured specimens in a Q2000 device of TA Instruments (New Castle, DE, USA). The weight of the specimen, placed in the aluminum pans, was of about 10 mg. Measurements were running from -50 ºC to 250 ºC with 10 ºC/min heating rate under steady nitrogen flushing (25 ml/min). In addition, the crosslinking in each step of the cure schedule was checked by isothermal DSC scans.

Parallel plate rheometry

The chemorheology of the samples of various EP/ESO compositions was investigated in a dynamic stress rheometer (RS 500 from Rheometrics Scientific, Piscataway, NJ, USA). Isothermal tests were done at T= 80, 100 and 120 ºC, respectively. The set parameters were: strain: 10 %, frequency: 10 rad/s. The gap between the plates of 25 mm diameter was kept constant, viz. 0.2 mm. The isothermal tests served to determine the gel time that was read at the crossing of the shear storage (G′) and loss moduli (G″).

Dynamic mechanical thermal analysis (DMTA)

DMTA traces were taken on rectangular specimens (30 ×5 × 3 mm; length × width ×thickness) in tension mode (span length: 20 mm) at 10 Hz using a DMA Q800 of TA Instruments (New Castle, DE, USA). Tests were run at constant amplitude (5 μm) using sinusoidal oscillation and under dynamic conditions in the temperature interval from -100 to 200 °C at a heating rate of 3 °C/min.

Thermomechanical analysis (TMA)

Specimens cut from the bulk samples and polished were tested in compression (penetration) mode in a TMA SS6000 device of Seiko Instruments (Chiba, Japan). TMA worked with an Exstar 6000 controller unit. A flat-tipped quartz rod of 3 mm diameter was pressed with 100 mN against the specimen surface. The temperature in the oven was raised from room temperature (RT, in some cases from -50 ºC) with a rate of 3 ºC/min until T=150 ºC. From the TMA traces

the coefficient of linear thermal expansion (CTE) was determined in both the glassy and rubbery states (i.e. below and above the actual T_g of the sample).

Thermogravimetrical analysis (TGA)

Samples taken from the bulk materials were subjected to TGA in nitrogen atmosphere (30 ml/min) using a TGA 7 device of PerkinElmer (Norwalk, CN, USA). The weighted material was few mg. Tests were run with 15 ^{o}C/min rate in the range from RT up to 600 ^{o}C. From the TGA and derivative TGA (DTGA) curves the temperatures at weight loss 2 and 10 wt.% were read, and the char yield was given by the residue at T=600 ^{o}C. The DTGA curves served to establish at what temperature is the weight loss rate the highest. In order to get a deeper insight in the thermal degradation process, more exactly to determine the activation energy of the thermal decomposition, TGA tests were performed on the sample series additionally also with 5 and 10 ^{o}C/min to calculate the activation energy.

3. RESULTS AND DISCUSSION

3.1. Curing

Figure 1 displays characteristic dynamic DSC scans. One can recognize a doubling in the curing exothermal peak for EP/ESO=50/50 and =25/75. The high temperature shoulder or peak is due to the ESO, the curing of which occurs at markedly higher temperature than the neat EP. This feature is well documented in the literature [14]. With increasing ESO content the cure enthalpy was reduced as follows: EP/ESO=100/0 – 335 J/g; 75/25 – 305 J/g; 50/50 - 230 J/g; 25/75 – 220 J/g; 0/100 - 209 J/g.

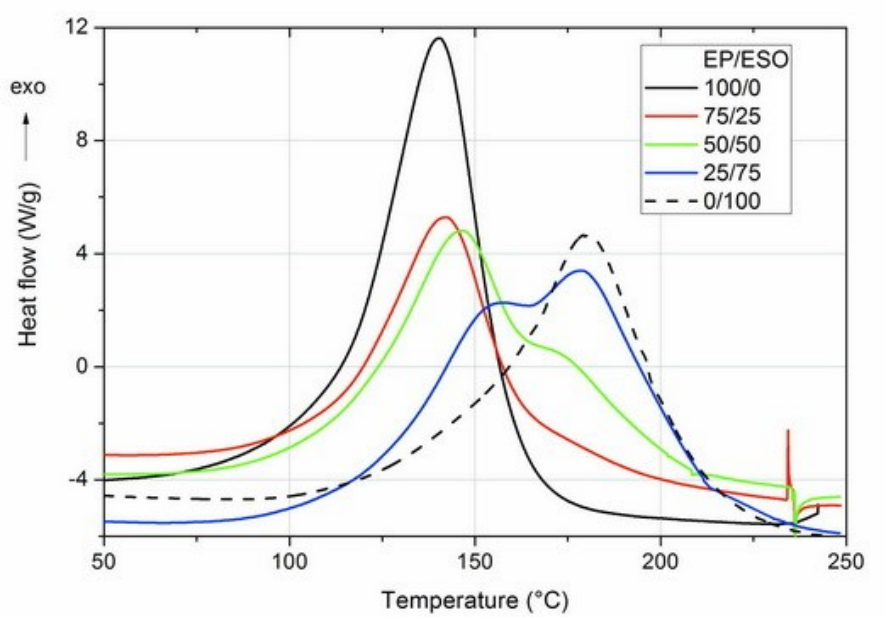

Figure 1: Dynamic DSC traces on curing of the EP/ESO formulations

The conversion (α) vs temperature curves, constructed based on the dynamic DSC scans, are shown in Figure 2. Their courses demonstrate well the temperature delay caused by increasing amount of ESO.

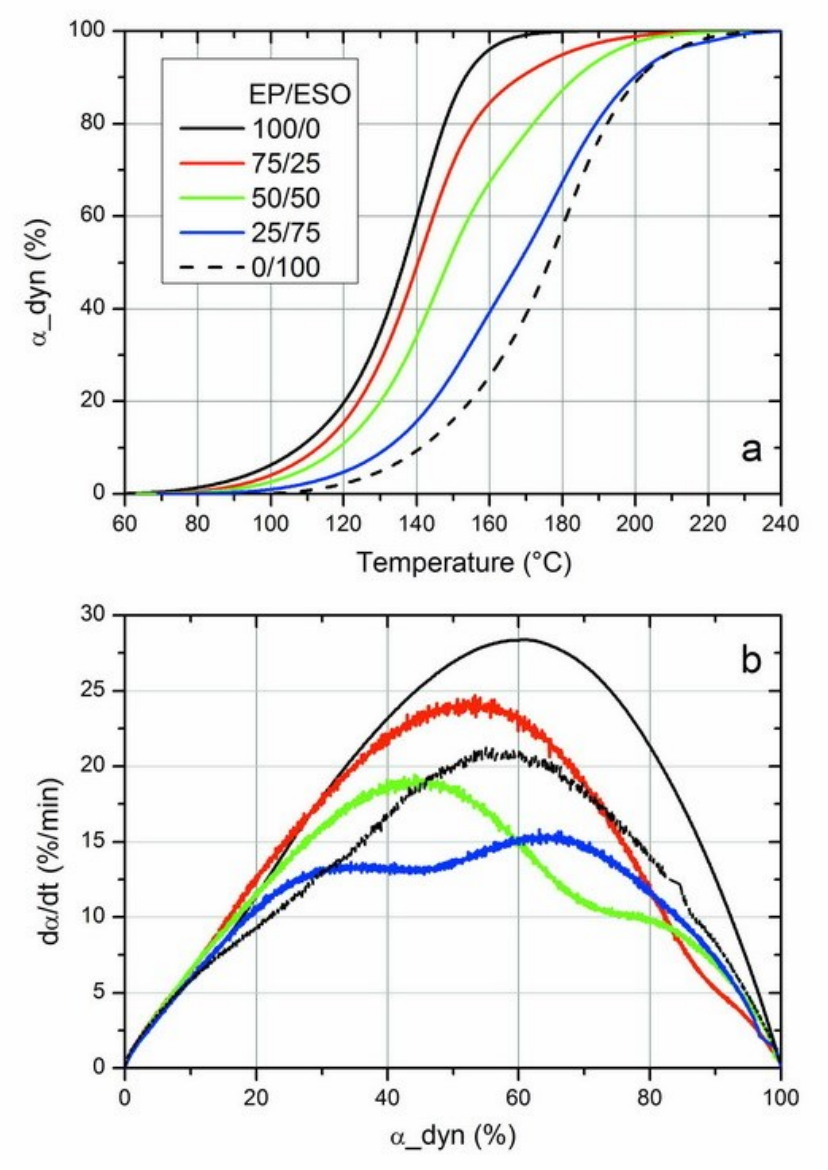

Figure 2: a) Conversion (α) vs temperature and b) conversion rate (dα/dt) vs conversion (α) traces derived from the dynamic DSC scans for the EP/ESO compositions

The conversion rate (dα/dt) vs conversion traces in Figure 2b highlight the ESO caused change in curing.

In Figure 3a and 3b the dα/dt vs time (t) and dα/dt vs conversion (α) traces are shown for the curing steps I, II and III. The related traces pinpoint that almost complete conversion was achieved after steps I and II. On the other hand, the degree of conversion of the EP/ESO compositions changed as a function of the composition prominently in the cure sections I and II. With increasing amount of ESO in the blend the conversion in step II increased compared to I. Based on the information in Figure 3 one can claim that the cure schedule selected was

appropriate for the EP/ESO hybrids.

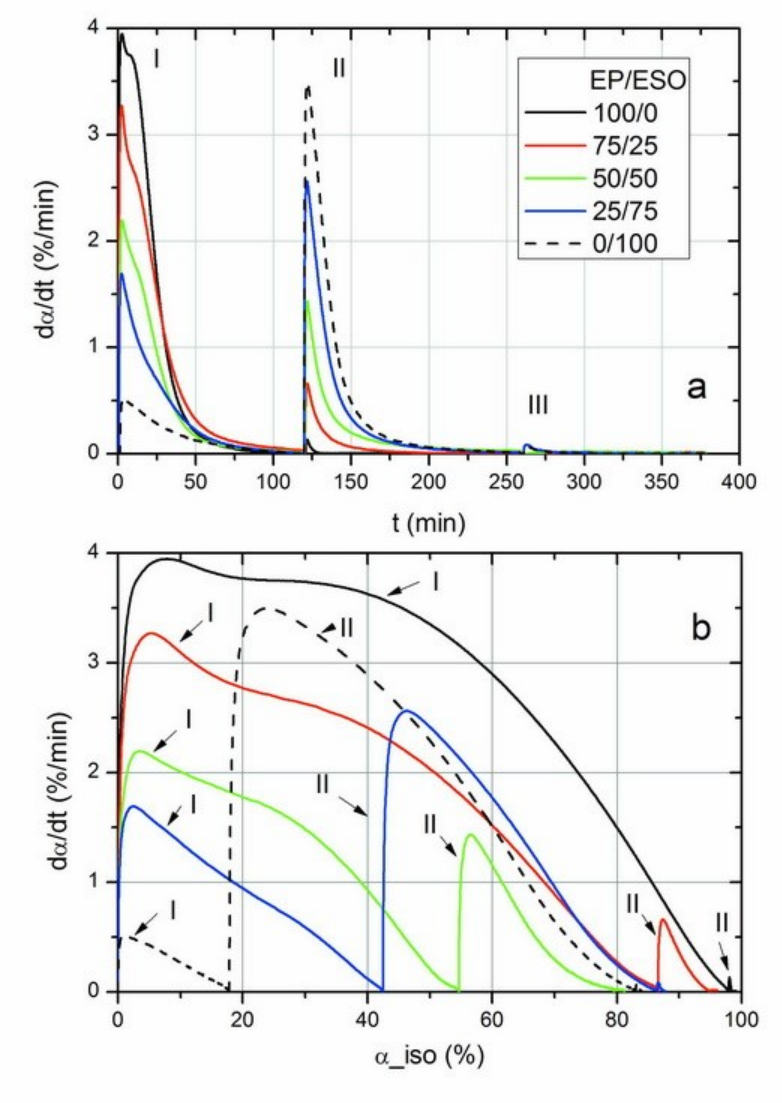

Figure 3: a) Conversion rate (dα/dt) vs time (t) and b) conversion rate (dα/dt) vs conversion (α) traces derived from the isothermal DSC scans for the EP/ESO compositions. Note: I, II and III refer to the isothermal holding for 2 hours at T=100, =140 and =180 ºC, respectively

3.2. Gelling

As an example for the original rheometer plots that one of the neat ESO (i.e. EP/ESO=0/100) measured at T= 140 ºC was selected (Figure 4).

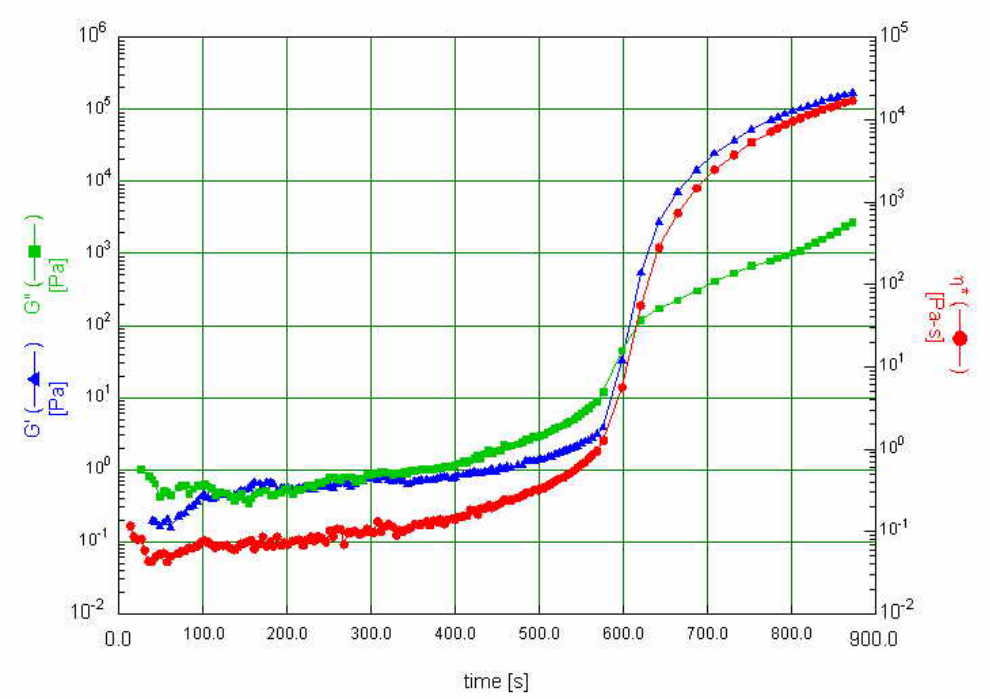

Figure 4. Change in the G′, G″ and complex viscosity (η*) as a function of time during the ESO (EP/ESO=0/100 system) curing at T= 140 °C,

The gel time (t_{gel}) values determined for the reference materials and blends at T=100, =140 and =180 °C are summarized in Table 1.

Table 1: Gel time data of the hybrid resins at various temperatures (mean data from 3 parallel tests) and activation energy (E_a) of gelling for the resins studied.

EP/ESO composition (wt.%/wt.%)	$t_{gel\ 100°C}$ (s)	$t_{gel\ 120°C}$ (s)	$t_{gel\ 140°C}$ (s)	E_a (kJ/mol)
100/0	1024	290	199	52.9
75/25	1261	379	201	59.0
50/50	2050	618	240	66.4
25/75	2688	787	283	72.1
0/100	5746	1772	600	72.3

The t_{gel} data in Table 1 clearly show that gelling takes place earlier with increasing temperature and with decreasing ESO content in the blends. The temperature dependence of the gel time is usually approximated by an Arrhenius-type function:

$$t_{gel}=C\cdot e^{Ea/RT} \quad (1)$$

where C is a constant (pre-exponential factor), Ea is the activation energy, R is the universal gas constant (8.135 $J(K\cdot mol)^{-1}$) and T is the absolute temperature of the curing.

The above equation can be linearized as follows:

$$\ln(t_{gel})=\ln C + E_a/(RT) \quad (2)$$

and thus by plotting $\ln(t_{gel})$ as a function of 1/T, i.e. reciprocal absolute temperature of curing, both the C and E_a can be determined. This is shown on example of the EP/ESO hybrids in Figure 5.

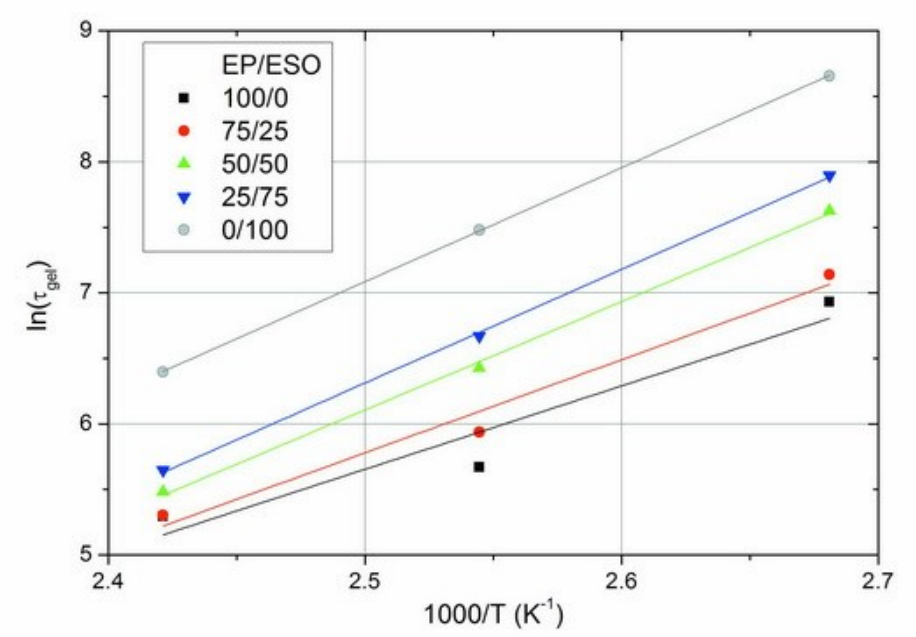

Figure 5. Determination of the activation energy of gelling.

The E_a data, also listed in Table 1, demonstrate that the activation energy increased with increasing amount of ESO for the anhydride cured EP/ESO blends. The E_a value, deduced for anhydride cured ESO is somewhat higher than that one reported for cationically cured ESO (63 kJ/mol) [21].

3.2. Tg and DMTA behavior

The T_g data were read from dynamic DSC curves taken from the cured materials (Figure 6) and summarized in Table 2. With increasing amount of ESO the T_g decreased in accordance with former results [6,8-9,14].

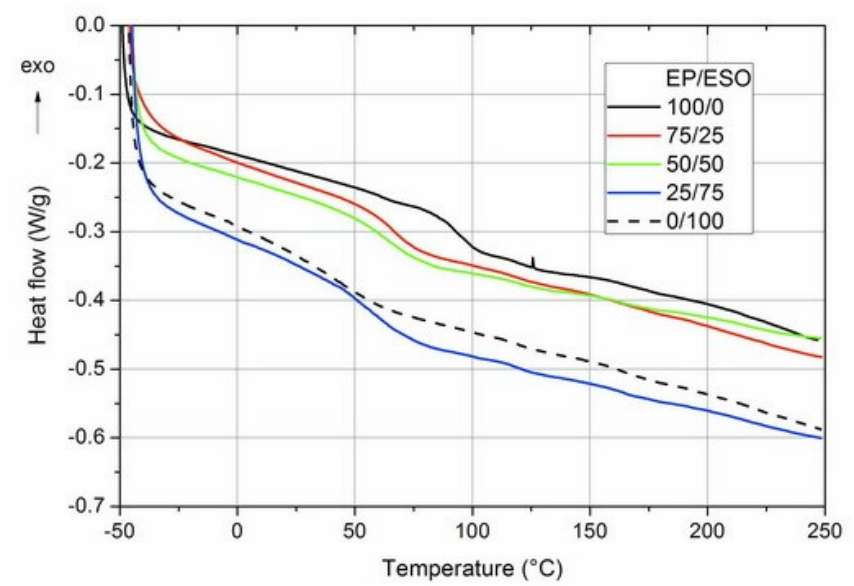

Figure 6: Dynamic DSC traces taken on the cured EP/ESO hybrids

The DMTA traces in form of storage modulus (E') and mechanical loss factor (tan δ) vs time are depicted in Figure 7. As expected, based on the reactive diluent role of ESO, the stiffness in the glassy state of the EP/ESO compositions decreased with increasing amount of ESO. Interestingly, this was not accompanied with a large change in the peak position of the tan δ transition what was expected according to the DSC results. By contrast, the ESO-caused plastification effect was well reflected by the change in the position of the loss modulus (E'') and even better with respect to the initial drop in E'. The latter, denoted as E'_{onset}, was read at the intersection of lines drawn to the flanks of E' at the T_g step. All the related Tg values are listed in Table 2.

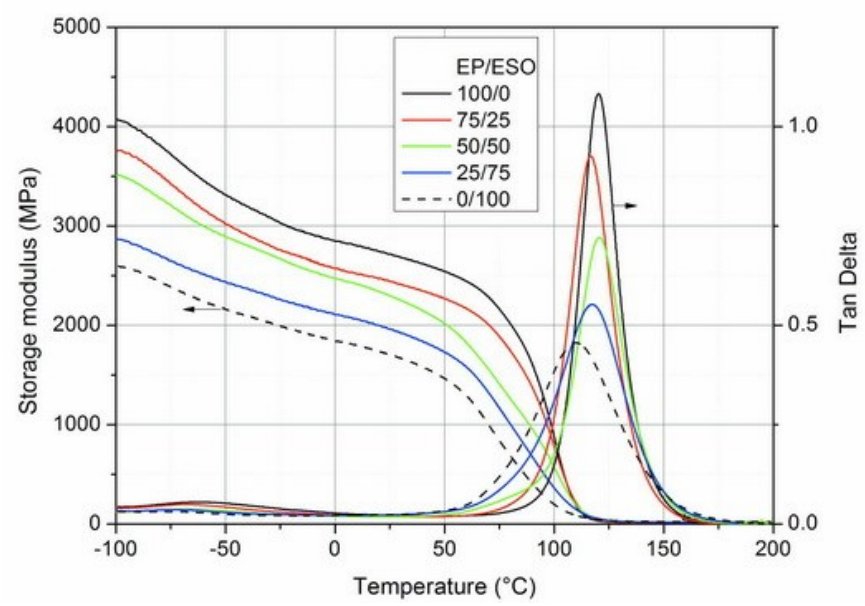

Figure 7. DMTA traces of the EP/ESO resin blends: storage moduli (continuous lines) and tanδ (dashed lines) vs temperature

Table 2. Glass transition temperature (T_g) data from DSC and DMTA (peak temperatures of tan δ and E″ and onset of E′ drop) and E′ data at RT ($E'_{25°C}$)

EP/ESO composition (wt.%/wt.%)	T_g (DSC) (°C)	T_g (DMTA) (°C)			$E'_{25°C}$ MPa
		tan δ	E″	E'_{onset}	
100/0	90	120	108	82	2722
75/25	65	117	102	81	2445
50/50	59	121	107	67	2301
25/75	53	118	92	60	1958
0/100	40	110	83	55	1705

3.3. Thermomechanical analysis (TMA)

Figure 8 shows the thickness change as a function of temperature for the EP and ESO references and EP/ESO hybrids. In the related traces one can resolve two linear sections: that one at lower temperatures represents the linear thermal expansion in the glassy, whereas that one at the high temperature flank the thermal expansion in the rubbery state. The run of the trace between the two linear sections is obviously linked with the T_g of the corresponding system.

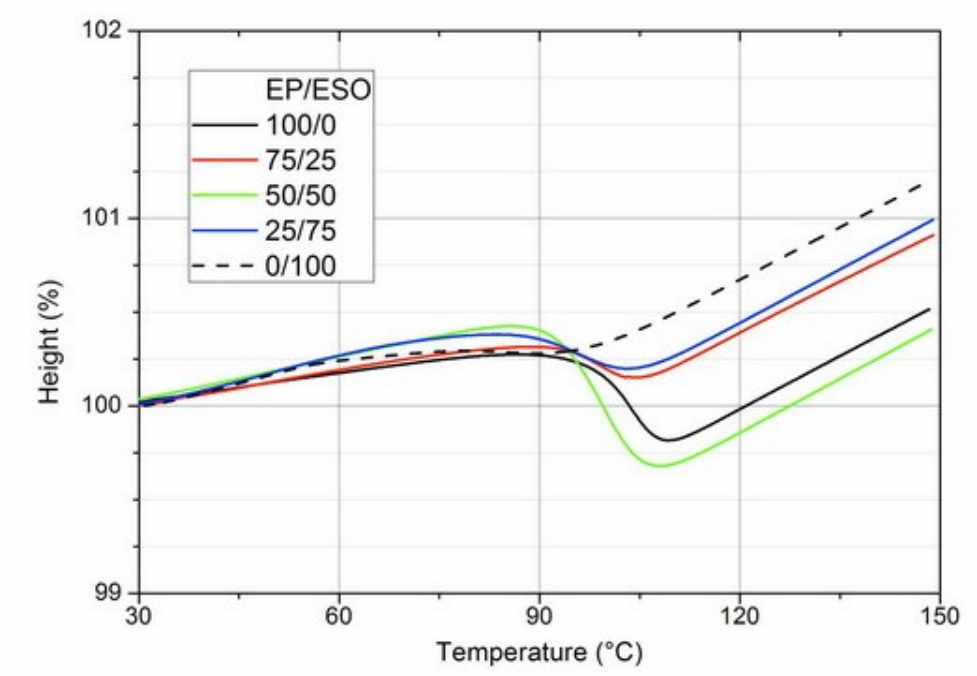

Figure 8. Height change of the samples as a function of temperature

Based on Figure 9 one can observe that with increasing ESO content the thermal expansion in the glassy (CTE_g) increases, whereas practically no change can be resolved in the rubbery state (CTE_r). Results from the TMA tests are listed in Table 3.

Table 3. TMA results (CTE) of the EP/ESO systems studied

EP/ESO composition (wt%/wt%)	CTE_g (ppm/°C)	CTE_r (ppm/°C)
100/0	50.4	188.9
75/25	61.7	181.3
50/50	75.9	190.8
25/75	89.8	189.2
0/100	92.5	185.6

Based on Figure 9 the CTE_g data can well be predicted by a linear regression as a function of the ESO content for the EP/ESO blends. It is noteworthy that all of our date are exactly one magnitude smaller than those reported by Lin and Park [15].

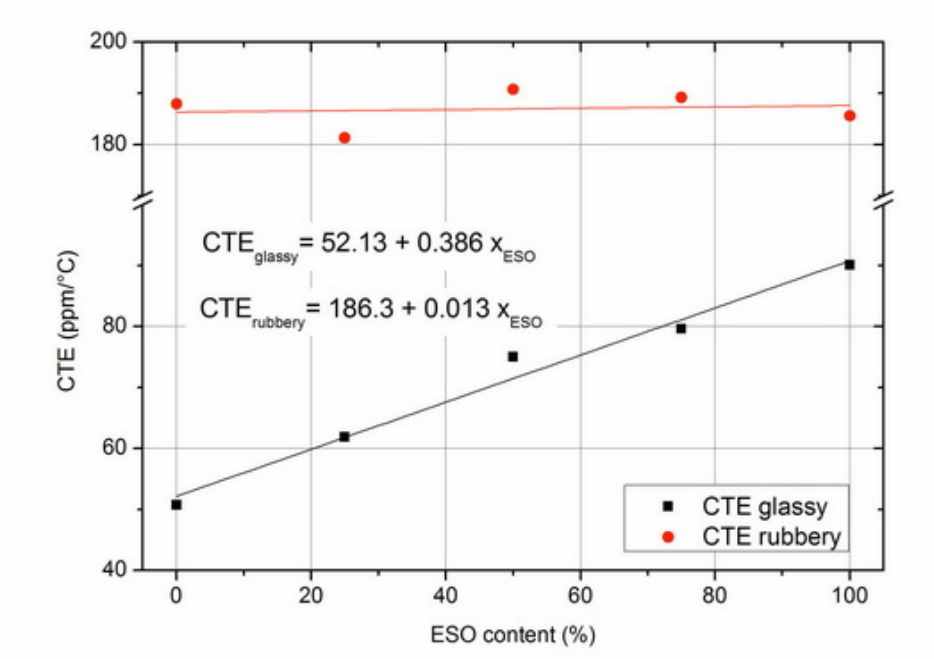

Figure 9. Change in the CTE data of the EP/ESO hybrids in the glassy and rubbery states as a function of ESO content. Note: in the linear regression fits the ESO content (x_{ESO}) is given in wt.%

3.4. TGA behavior

The TGA curves of the anhydride cured systems, when tested at 15 ºC/min heating rate, are shown in Figures 10a and 10b, respectively.

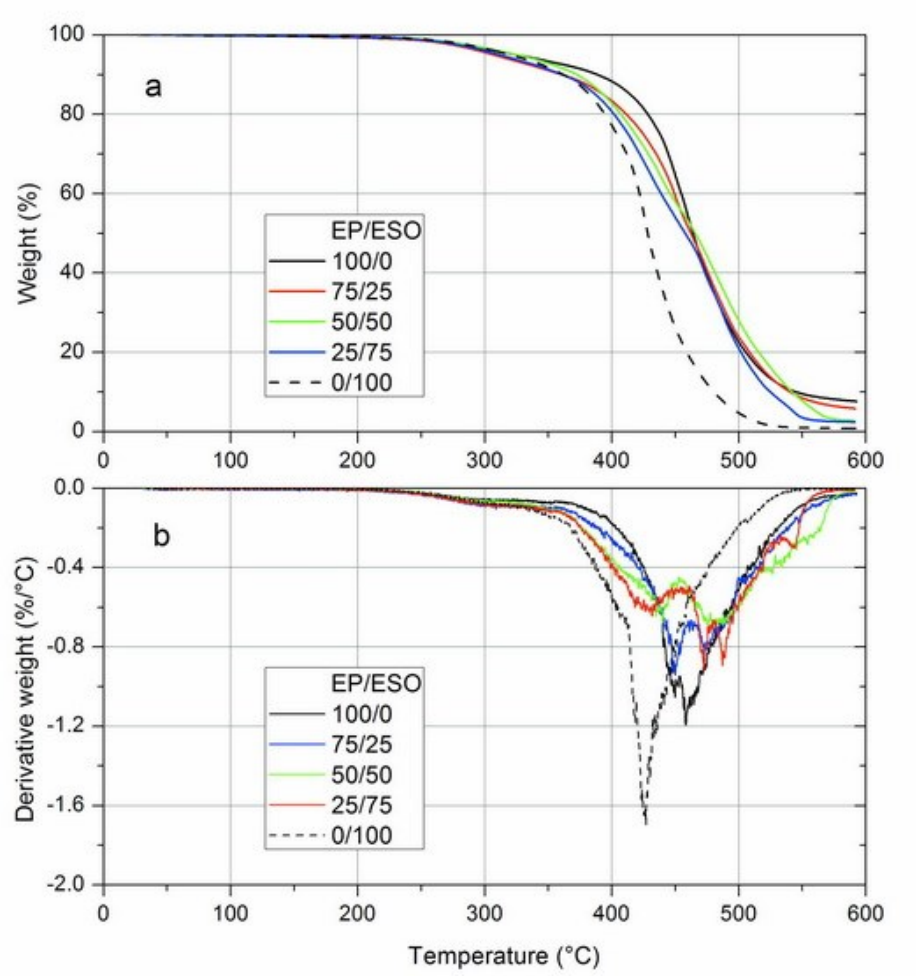

Figure 10. TGA (a) and DTGA (b) traces registered at 15 ºC/min heating rate for the EP/ESO systems

The initial thermal decomposition of the EP/ESO blends started earlier than that of the reference EP, but the ESO content had only a marginal effect in the starting phase. The char yield decreased, however, with increasing ESO content.

Based on Figure 10b one can say that the peak linked with the highest decomposition rate of EP splits in case of the EP/ESO blends. This peak doubling suggests more complex degradation process and hints for the presence of a highly inhomogeneous crosslinked structure.

The TGA behavior of the hybrids studied is characterized by the following parameters: temperatures where the weight loss was 2 and 10 wt.% ($T_{-2\%}$ and $T_{-10\%}$), respectively; temperature where the rate of the thermal decomposition was the highest (T_{peak}). This was read as the peak temperature in the DTGA traces, and char yield representing the final residue at T=600 ºC.

The related data are summarized in Table 4.

Table 4. TGA results of the anhydride-cured EP/ESO systems

EP/ESO composition (wt.%/wt.%)	$T_{-2\%}$ (^oC)	$T_{-10\%}$ (^oC)	T_{peak} (^oC)	Char yield (wt.%)
100/0	269	389	459	7.59
75/25	265	361	450 / 473	5.80
50/50	278	373	440 / 483.5	2.74
25/75	270	361	472 / 488	2.38
0/100	277	362	426	0.79

The T_{peak} data in Table 4 suggest that the kinetics of the thermal degradation was strongly influenced by the ESO content. Increasing ESO content practically did not affected $T_{-2\%}$, and somewhat reduced $T_{-10\%}$. With increasing ESO content the residual char was also reduced.

In order to calculate the activation energy ($E_{a,t}$) of the thermal decomposition TGA tests were run with two additional heating rates (β), viz. 5 and 10 ^{o}C/min, respectively.

The activation energy of thermal decomposition ($E_{a,t}$) can be calculated by the isoconversional method of Ozawa, Flynn and Wall (OFW) [22-24]. This is "model free" method which involves the measuring of the temperatures corresponding to fixed values of thermal decomposition from the TGA experiments at different heating rates. Plotting lnβ against 1/T in the form of

$$\ln\beta = \ln A - E_{a,t}/(RT) \quad (3)$$

should give straight lines and its slope is directly proportional to the activation energy ($-E_{a,t}/R$), where A is the pre-exponential factor, T is the absolute temperature, and R is the gas constant. If the determined activation energy is the same for the various values of weight losses then the existence of a single-step reaction can be concluded with certainty. On the contrary, a change of $E_{a,t}$ with increasing degree of decomposition is an indication of a complex reaction [24]. For the actual weights ("thermal conversion") the following values were considered: 75, 50 and 25 wt.% (i.e. weight losses 25, 50 and 75 wt.%, respectively).

Figure 11 shows the determination of the activation energy through the above equation on example of the EP/ESO=50/50 hybrid at different thermal conversions.

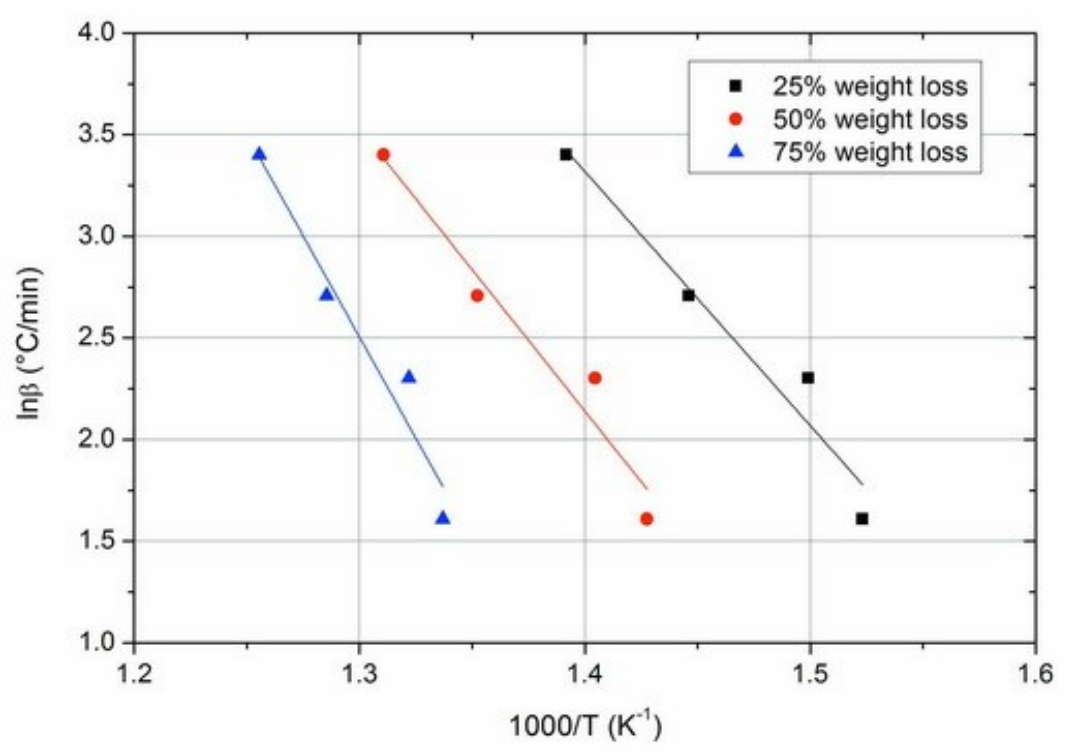

Figure 11. Determination of the activation energy ($E_{a,t}$) based on the OFW equation for the anhydride-cured EP/ESO=50/50 at different weight losses.

The results achieved by using the OFW method are summarized in Table 5.

Table 5. Activation energy ($E_{a,t}$) determined according to the OFW equation at different decompositions, viz. 25, 50 and 75 wt.%

EP/ESO composition (wt.%/wt.%)	$E_{a,t\ -25\%}$ (kJ/mol)	$E_{a,t\ -50\%}$ (kJ/mol)	$E_{a,t\ -75\%}$ (kJ/mol)
100/0	103.0	120.4	123.6
75/25	102.0	106.9	115.6
50/50	101.5	113.0	161.5
25/75	99.6	103.9	153.1
0/100	151.9	233.0	234.2

Data in Table 5 inform us that the activation energy can be treated as independent of the actual state of degradation (thermal conversion) in the best case only for EP/ESO=100/0 and =75/25. At higher ESO content the activation energy increased with increasing degradation. Accordingly,

the prerequisites of the OFW equation do not hold for the related systems anymore. This is due to the inhomonegous network structure formed which affected also the thermal decomposition.

CONCLUSION

Based on this work devoted to study the curing, gelling, thermomechanical and thermal degradation behavior of anhydride cured EP/ESO compositions the following conclusions can be drawn:

- curing was delayed as a function of temperature with increasing amount of ESO. The related DSC traces showed a peak doubling assigned to the separate curing of the EP and ESO. Proper curing of the EP/ESO formulations covering the whole composition range was achieved by a cure program composed of three sections, viz. holding at T=100, =140 and =180 ^{o}C, respectively, for 2 h each

- gel times determined at the above temperatures increased with increasing amount of ESO in the compositions. This was accompanied with an increase in the activation energy of gelling

- EP/ESO hybrids were transparent and exhibited a single glass transition. The related temperature decreased with increasing ESO content and depended on its determination modes (DSC, DMTA characteristics). ESO, acting as reactive plasticizer in EP, reduced the stiffness in the glassy state, as well.

- coefficient of linear thermal expansion in the glassy state increased with increasing amount of ESO in the blends. By contrast, its value was practically constant in the rubbery state.

- incorporation of ESO reduced the onset of thermal decomposition of the EP/ESO blends and its amount influenced the decomposition that occurred in two steps. They can be traced to the ESO and EP rich phases, respectively. The activation energy, determined by the OFW method, increased with the decomposition degree for most of the blends. Nonetheless, the activation energy of thermal decomposition increased with increasing amount of ESO

Acknowledgements

The research leading to these results has received funding from the Hungarian Research Funds (OTKA, n° NK 83421) and European Union's Seventh Framework Programme (FP7/2007-2013) for the Clean Sky Joint Technology Initiative under grant agreement n° 298090. It is also connected to the scientific program of the "Development of quality-oriented and harmonized

R+D+I strategy and functional model at BME", supported by the New Hungary Development Plan (Project ID: TÁMOP-4.2.1/B-09/1/KMR-2010-0002). The authors thank Mr. H. Apostolov for his help in the experimental work.

References

1 M.A.R. Meier, J.O. Metzger and U.S. Schubert, Chem. Soc. Rev., **36**, 1788 (2007).

2 J.-M. Raquez, M. Deléglise, M.-F. Lacrampe and P. Krawczak, Progr. Polym. Sci., **35**, 487 (2010).

3 S.N. Khot, J.J. Lascala, E. Can, S.S. Morye, G.I. Williams, G.R. Palmese, S.H. Kusefoglu and R.P. Wool, J. Appl. Polym. Sci., **82**, 703 (2001).

4 S.Grishchuk and J. Karger-Kocsis, Expr. Polym. Lett. **5**, 2 (2011)

5 S.Grishchuk and J. Karger-Kocsis, J. Mater. Sci., **47**, 3391 (2012)

6 S.G. Tan and W.S. Chow, Polym.-Plast. Techn. Eng., **49**, 1581 (2010)

7 C.S. Ilardo and B.O. Schoepfle, Ind. Eng. Chem., **52**, 323 (1960).

8 R. Raghavachar, R.J. Letasi, P.V. Kola, Z. Chen and J.L. Massingill, J. Am. Oil Chem. Soc., **76**, 511 (1999).

9 J. Zhu, K. Chandrashekhara, V. Flanigan and S. Kapila, J. Appl. Polym. Sci., **91**, 3513 (2004)

10 D. Ratna, Polym. Intern, **50**, 179 (2001)

11 P. Czub, Macromol. Symp., **245-246**, 533 (2006)

12 H. Miyagawa, M. Misra, L.T. Drzal and A.K. Mohanty, Polym. Eng. Sci., **45**, 487 (2005)

13 A.P. Gupta, S. Ahmad and A. Dev, Polym. Eng. Sci., **51**, 1087 (2011)

14 F.I. Altuna, L.H. Espósito, R.A. Ruseckaite and P.M. Stefani, J. Appl. Polym. Sci., **120**, 789 (2011)

15 F.-L. Jin and S.-J. Park, Polym. Intern. **57**, 577 (2008)

16 N.W. Manthey, F. Cardona and T. Aravinthan, J. Appl. Polym. Sci., **125**, E511 (2012)

17 A.E. Gerbase, C.L. Petzhold and A.P.O. Costa, J. Am. Oil Chem. Soc., **79**, 797 (2002).

18 S.G. tan and W.S. Chow, Expr. Polym. Lett., **5**, 480 (2011)

19 A.R. Mahendran, G. Wuzella, A. Kandelbauer and N. Aust, J. Thermal. Anal. Calorim., **107**, 989 (2012)

20 D.S. Martini, B.A. Braga and D. Samios, Polymer **50**, 2919 (2009)

21 F.-L. Jin and S.-J. Park, J. Ind. Eng. Chem., **13**, 808 (2007)

22 T. Ozawa, Bull. Chem. Soc. Jpn. **38**, 188 (1965)

23 J. Flynn, L.A. Wall, J. Polym. Sci. Part B: Polym. Lett. **4**, 232 (1966)

24 K. Chrissafis, K.M Paraskevopoulos, E. Pavlidou and D. Bikiaris, Thermochim. Acta **485**, 65 (2009)